water

MDPI

Article

Service Pressure and Energy Consumption Mitigation-Oriented Partitioning of Closed Water Distribution Networks

Enrico Creaco *, **Carlo Giudicianni** and **Alessandro Tosco**

Dipartimento di Ingegneria Civile e Architettura, Università Degli Studi di Pavia, 27100 Pavia, Italy; carlo.giudicianni@unipv.it (C.G.); alessandro.tosco01@universitadipavia.it (A.T.)
* Correspondence: creaco@unipv.it; Tel.: +39-(0)382-985317

Abstract: This paper presents the partitioning of the closed water distribution network (WDN) serving the city of Pavia, Italy. As a thus far poorly explored aspect in the scientific literature, clustering for the definition of size and extension of district metered areas (DMAs) and of inter-DMA boundary pipes is performed by ensuring that the DMAs respect the altimetric areas of the WDN by leaning on a modified formulation of modularity. To define the boundary pipes to be closed or alternatively fitted with a flow meter for the monitoring of DMA consumption, the dividing is performed with an innovative heuristic algorithm. This technique operates by sequentially implementing the boundary closures that do not cause significant head losses, to obtain an approximation of the Pareto front in the trade-off between number of flow meters installed and WDN reliability. In the last part of the work, the pumps present in the network are assumed to be equipped with the variable speed drive, and their hourly settings are optimized to regulate service pressure. Overall, WDN partitioning and pump setting optimization are proven to mitigate the service pressure and energy consumption of the WDN, offering evident and attractive benefits up to about 50% for water utilities.

Keywords: closed water distribution network; partitioning; altimetric areas; optimization; pump; energy consumption; service pressure

check for updates

Citation: Creaco, E.; Giudicianni, C.; Tosco, A. Service Pressure and Energy Consumption Mitigation-Oriented Partitioning of Closed Water Distribution Networks. *Water* **2023**, *15*, 3218. https://doi.org/10.3390/w15183218

Academic Editor: Pankaj Kumar

Received: 8 August 2023
Revised: 31 August 2023
Accepted: 8 September 2023
Published: 10 September 2023

Copyright: © 2023 by the authors. Licensee MDPI, Basel, Switzerland. This article is an open access article distributed under the terms and conditions of the Creative Commons Attribution (CC BY) license (https://creativecommons.org/licenses/by/4.0/).

1. Introduction

In light of the ever-increasing climate crisis and demographic problems, which place great stress on urban infrastructures, the efficient management of water distribution networks (WDNs) represents a crucial task in the pursuit of a more sustainable and efficient use of water/energy, and in general a more sustainable development strategy. In this regard, besides guaranteeing water supply at adequate pressure service and quality, one of the main challenges faced by water utilities is the minimization of water losses and energy consumption. Incidentally, WDNs represent the largest share of energy consumption in the water sector, which in turn corresponds to 4% of total global electricity consumption [1].

Within this context, one of the most explored and adopted strategies is partitioning, namely, the definition of district metered areas (DMAs) [2] into which to subdivide the WDN. Notably, by simplifying water budget computation, and consequently leakage detection/identification, efficient WDN partitioning also contributes to a reduction in the overall energy wastage of the non-revenue water (i.e., for treatment plants and pumping stations). Furthermore, over the years, researchers and practitioners have investigated the manifold benefits of adopting WDN partitioning, i.e., simplified pressure management [3], speedier repair interventions [4], improved protection against contaminants [5], and better treatment of abnormal water demand requests [6]. To sum up, smaller monitored areas reduce the topological and operational complexity of the WDN, allowing water companies to efficiently work with more tamable operational and management programs.

In this regard, differential pressure management in DMAs allows for effective leakage control [7], especially for large WDNs featuring high-service pressure zones and/or a steep altimetric profile. Indeed, the sub-zoning of the WDN according to the spatial distribution of daily average pressure head leads to simplified and more targeted schedule setting for pressure-reducing valves and pumping stations. Accordingly, in high- and low-pressure areas, it is possible to achieve significant water loss savings and energy consumption mitigation without compromising the minimum service level in other areas, and with a more balanced pressure distribution in the WDN.

Generally, partitioning is carried out in two phases, i.e., clustering and dividing [8]. Clustering, typically performed using graph theory techniques, aims to define the number and extension of the DMAs, balancing their size/features and minimizing the number of boundary pipes connecting them. The dividing phase consists of optimally located gate valves/flow meters on the boundary pipes, achieved by minimizing the economic investment/hydraulic performance deterioration and maximizing the managerial/control/operational benefit (see [8] for an extensive critical review).

A widely adopted metric in the context of WDN partitioning ([9–11]) is modularity [12], which effectively quantifies the goodness of network subdivision into communities (in terms of balanced cluster sizes and few boundary links). In this regard, the recently developed modularity-based procedure by Creaco et al. 2023 [13], originally conceived for a dual WDN topology (segment/valve graphs), can be used for the clustering of the standard node/pipe topology. Notably, besides the minimization of the number of boundary pipes, this procedure also allows for the definition of internally uniform DMAs in terms of nodal ground elevation, in such a way that districts pander the altimetric areas of the WDN, thus facilitating pressure regulation/leakage reduction, and consequently, energy savings. In fact, spatially close and interconnected nodes with similar ground elevations typically feature similar service pressure values, and are therefore prone to being grouped into the same pressure zone. Therefore, the clustering of these nodes into the same DMA leads to effective WDN partitioning for pressure regulation. This represents an important but not deeply investigated partitioning criterion (e.g., see [14,15]), which motivated the present work, in which a novel heuristic procedure is also presented for the selection of the boundary pipes to close or to alternatively fit with a flow meter in the dividing phase. To mitigate the problems of excessive consumption of electric power, which are nowadays very much targeted at pumping stations [16,17] and other contexts [18,19], the work also proposes installation of variable speed drives [20] at system pumps and pump hourly setting optimization based on a bespoke algorithm for closed WDNs, with no intermediate tanks between sources and end users.

The following sections describe a real Italian case study, the methodology adopted, and its application. The paper ends with a critical discussion of the results.

2. Case Study

The real WDN of Pavia, Northern Italy, was the case study considered in this paper. This WDN includes 12 source nodes, representative of groundwater wells with elevation ranging between 55 m and 88.1 m, 4277 demand nodes with ground elevation ranging from 57.19 m to 86.11 m, 4733 pipes with diameter ranging between 25 mm and 500 mm, and a Hazen–Williams roughness coefficient between 130 and 150, with 12 pumps drawing water from the wells. The total length of the WDN is about 213 km. Figure 1 shows the layout of the WDN and the present altimetric areas.

The model of the WDN is available in the EPANET 2.2 [21] environment.

The total average demand of the WDN adds up to about 347 L/s. In the model, the daily pattern of the hourly demand factor C_d shown in Figure 2 is considered, in order to simulate the daily operation of the WDN in an extended simulation period.

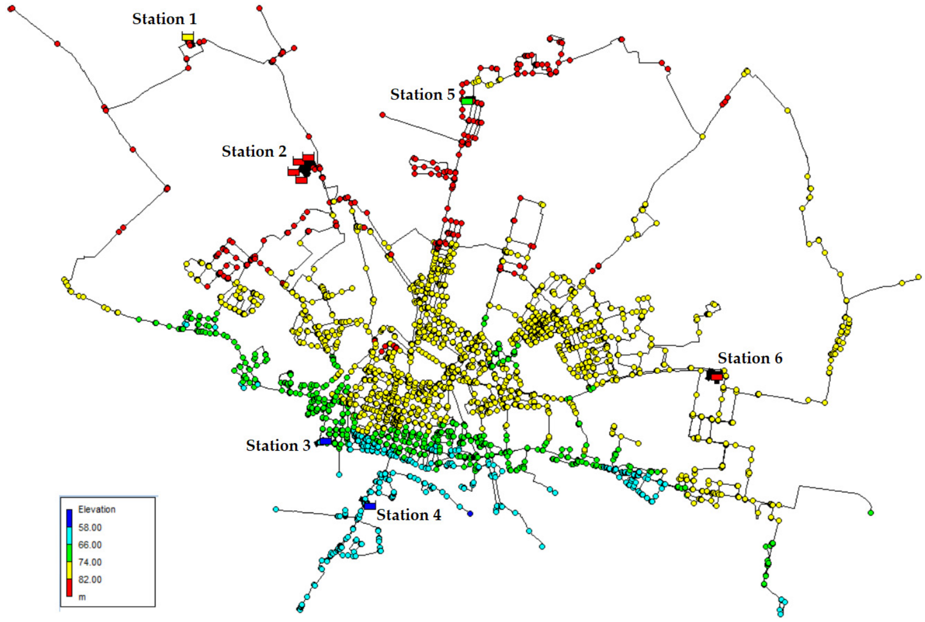

Figure 1. WDN of Pavia and nodal elevations.

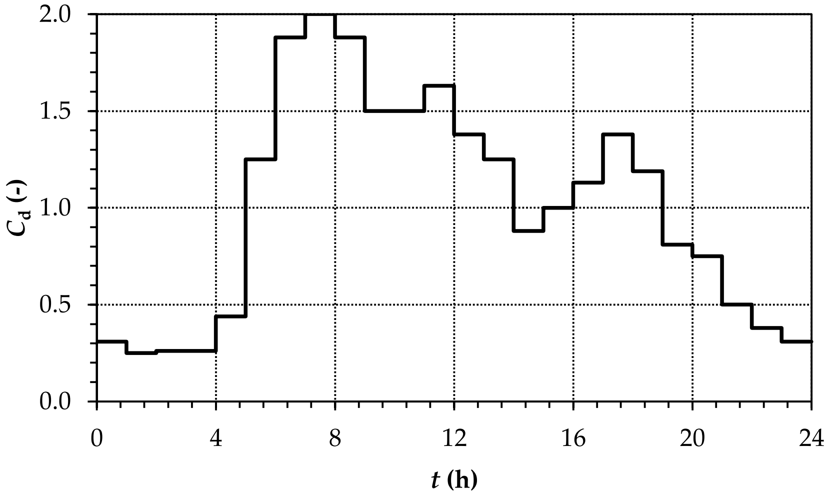

Figure 2. Daily pattern of hourly demand factor C_d.

The twelve fixed-speed pumps present in the model are grouped in six pumping stations, as shown in Figure 1. Inside each pumping station, a single pump model is present, with a variable number of units between 1 and 4. The main characteristics of the pump model present in each pumping station in terms of maximum water discharge and head are reported in Table 1.

Table 1. Characteristics of the pumping stations in terms of number of pumps and maximum water discharge Q_{max} and head H_{max}.

Station ID	Station Name	Number of Pumps	Q_{max} (L/s)	H_{max} (m)
1	Villalunga	1	50	80
2	Nord	4	144	47
3	Libertà	1	38	85
4	Borgo Ticino	1	38	85
5	Mirabello	1	50	80
6	Est	4	144	47

3. Materials and Methods

The methodology used in this paper is based on the following elements (e.g., see flowchart in Figure 3):

- Partitioning (clustering and dividing) of the WDN;
- Optimization of the hourly settings of the pumping stations present in the WDN.

The methodological elements listed above are described in the following subsections.

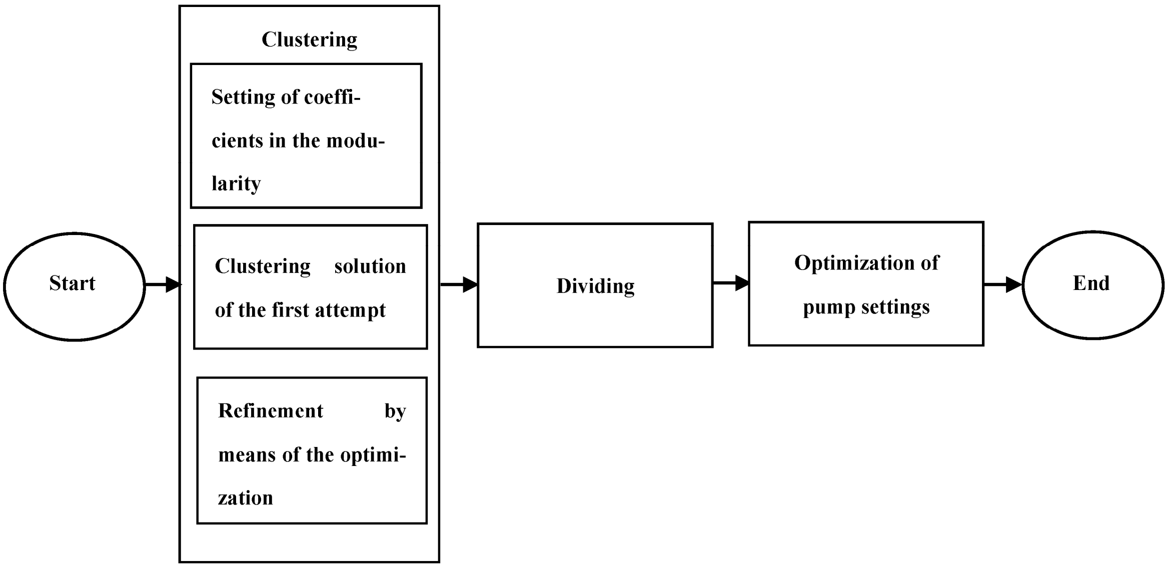

Figure 3. Flowchart of the methodology.

3.1. WDN Partitioning

3.1.1. Clustering

The methodology proposed by Creaco et al. 2023 [13] was used for the clustering, that is, for the definition of the size of the DMAs and for the identification of the inter-DMA boundaries. Though originally conceived for the dual topology based on WDN segments and isolation valves, the methodology is applied here to the standard topology based on nodes and pipes. This methodology is based on a novel formulation of modularity Q, obtained by subtracting three terms from the unity, related to the ratio of the number of boundary pipes to the number of WDN pipes, the uniformity of a selected property between DMAs, and the uniformity of another selected property inside each DMA, respectively. This formulation is expressed by the following relationship [13]:

$$Q = 1 - \sum_{i=1}^{3} \alpha_i H_i \quad (1)$$

in which H_i and α_i are the three terms described above, and their respective weighing coefficients. The terms H_i are calculated with the following relationships [13]:

$$H_1 = \frac{n_b}{n_p} \quad (2)$$

$$H_2 = \frac{1}{U_{tot}^2} \sum_{i=1}^{M} (U_i)^2 \quad (3)$$

$$H_3 = \frac{\sum_{i=1}^{M} \sum_{j=1}^{n(i)} \left[\left(u_{i,j} - \overline{u_i} \right)^2 / n(i) \right]}{(u_{max} - u_{min})^2} \quad (4)$$

in which n_b and n_p are the number of boundary pipes and the total number of pipes, respectively. U_i is the property to be made uniform between the DMAs (for instance, DMA demand), while U_{tot} is the sum of U_i in all the M DMAs. With reference to the property to be made uniform inside each segment, e.g., ground elevation, $u_{i,j}$ is the property values in the j-th of the $n(i)$ nodes of the i-th DMA. Then, $\overline{u_i}$ is the mean value of $u_{i,j}$ in the i-th DMA, while u_{max} and u_{min} are the maximum and minimum values of $u_{i,j}$ in the whole WDN, respectively.

The structure of Equations (1–4) is such that modularity Q decreases when the number of boundary pipes, the heterogeneity of demands between DMAs, and the heterogeneity of nodal ground elevations inside each DMA grow.

The search for optimal clustering configurations in terms of modularity is performed in two steps:

- Construction of a configuration of the first attempt with the desired number M of clusters;
- Refinement of the configuration by means of an algorithm inspired by simulated annealing to search for a configuration with a better value of Q, the number M of clusters being the same.

Simulated annealing [22] is a probabilistic technique for approximating the global optimum in an optimization problem.

As far as the weights α_i are concerned [13], we recommend that a sensitivity analysis be performed by varying them within the range [0, 2], while making sure that their sum stays equal to 2. Based on the configurations obtained during the sensitivity analysis, the ultimate clustering solution can be chosen.

The methodology set up by Creaco et al. 2023 [13] was developed in the Matlab 2023a environment [23].

3.1.2. Dividing

After the ultimate clustering solution is constructed as explained in Section 3.1.1, a decision must be made on which boundary pipes to close or alternatively fit with a flow meter, to monitor the instantaneous consumption of DMAs.

The works of Creaco et al. [13,24] recommend that the dividing be performed with a bi-objective optimization aimed at simultaneously minimizing the partitioning cost associated with the installation of flow meters and maximizing, under peak demand conditions, a surrogate for reliability, like the generalized resilience failure (GRF) index [25], which is given by the sum of the resilience I_r and failure I_f indices, expressed as follows [25]:

$$I_r = \frac{\max\left(\mathbf{q}_{\mathbf{user}}^{\mathbf{T}}\mathbf{H} - \mathbf{d}^{\mathbf{T}}\mathbf{H}_{\mathbf{des}}, 0\right)}{\mathbf{Q}_0^{\mathbf{T}}\mathbf{H}_0 + \mathbf{Q}_{\mathbf{p}}^{\mathbf{T}}\mathbf{H}_{\mathbf{p}} - \mathbf{d}^{\mathbf{T}}\mathbf{H}_{\mathbf{des}}} \quad (5)$$

$$I_f = \frac{min\left(\mathbf{q}_{\mathbf{user}}^{\mathbf{T}}\mathbf{H} - \mathbf{d}^{\mathbf{T}}\mathbf{H}_{\mathbf{des}}, 0\right)}{\mathbf{d}^{\mathbf{T}}\mathbf{H}_{\mathbf{des}}} \quad (6)$$

in which $\mathbf{q}_{\mathbf{user}}$ and $\mathbf{d}$ are the vector of nodal outflows to users and user demands at demand nodes, respectively. $\mathbf{H}$ and $\mathbf{H}_{\mathbf{des}}$ are the vectors of nodal heads and desired heads for full outflow at demand nodes. Namely, the generic element H_{des} of $\mathbf{H}_{\mathbf{des}}$ can be calculated by summing the nodal ground elevation z and the desired pressure head h_{des}. $\mathbf{Q}_0$ and $\mathbf{H}_0$ are the vectors of source outflows and heads, respectively. Finally, $\mathbf{Q}_{\mathbf{p}}$ and $\mathbf{H}_{\mathbf{p}}$ are the vectors of pump flows and heads, respectively. GRF is an index ranging from -1 to 1, in which the larger values are associated with high-pressure heads at demand nodes, guaranteeing full satisfaction of user demands. While the negative values of GRF accounted for in I_f represent a power deficit in the WDN, the positive values of GRF accounted for in I_r represent the surplus of power, compared to the minimum power necessary for meeting user demands with suitable service pressure. The GRF is close to 1 when small head losses are present in the WDN under peak demand conditions. In the present work, GRF variations are calculated to analyze the power dissipation effects produced by the closure of boundary pipes in the dividing phase of WDN partitioning.

The present work proposes an efficient and effective way to tackle bi-objective optimization with the following iterative method, in which the number of flow meters is a surrogate for the partitioning cost.

At the beginning of the iterations (iteration 0), all boundary pipes are fitted with a flow meter (number n_f of flow meters = number n_b of boundary pipes). This configuration of flow meters is associated with the highest GRF = GRF_0.

Then, at iteration 1, the closure of one boundary pipe at a time is tested to identify which boundary closure yields the lowest decrease in GRF from the configuration of flow meters at $k = 0$. The configuration of flow meters obtained in correspondence to the lowest decrease in GRF is the final configuration for iteration 1, with $n_f = n_b - 1$ and GRF= GRF_1.

At iteration 2, while keeping closed the boundary pipe identified at iteration 1, the closure of an additional boundary pipe at a time is tested to identify which boundary closure yields the lowest decrease in GRF from the configuration of flow meters found at the end of iteration 1. The configuration of flow meters obtained in correspondence to the lowest decrease in GRF is the final configuration for iteration 2, with $n_f = n_b - 2$ and GRF = GRF_2.

The iterations then continue in a similar way. At the generic k-th iteration, while keeping the boundary pipes identified at iterations from 1 to $k-1$ closed, the closure of one additional boundary pipe at a time is tested to identify which boundary closure yields the lowest decrease in GRF from the configuration of flow meters at the end of the $k-1$-th iteration. The configuration of flow meters obtained in correspondence to the lowest decrease in GRF is the final configuration for the generic k-th iteration, with $n_f = n_b - k$ and GRF = GRF_k.

The iterations end when no additional boundary pipe can be closed in the WDN without causing topological disconnections from the source(s), or when the pressure drops below the desired pressure head h_{des}.

By plotting the number n_f of flow meters installed as a function of the GRF, an effective and efficient approximation of the Pareto front in the trade-off between n_f and GRF, to be minimized and maximized respectively, is obtained. The Pareto front can also be plotted in the trade-off between the number of closed isolation valves on boundary pipes $N_{civ} = n_b - n_f$ and GRF, for both to be maximized.

If no topological disconnections and pressure drops below h_{des} are encountered while reducing the number of flow meters from $n_f = n_b$ down to $n_f = 0$, the number N_c of WDN configurations explored in the present iterative algorithm is:

$$N_c = \sum_{i=0}^{n_b-1} (n_b - i) \tag{7}$$

which is much lower than the number of WDN configurations that would be explored in an optimization with evolutionary algorithms, such as the genetic algorithm (order of magnitude n_b^2). In fact, in the case of $n_b = 50$, the relationship (7) would yield $N_c = 1275 << n_b^2 = 2500$.

The iterative algorithm for the dividing was implemented in the Matlab® 2023a environment [23]. The hydraulic solver used for the evaluation of GRF at each iteration is the Epanet 2.2 toolkit developed by [26].

3.2. The Optimization of Pump Settings

In a closed WDN like that shown in Figure 1, each time instant of operation is independent of the others in the extended period simulation, due to the absence of variable level tanks. At each time instant of WDN operation, the pump settings can be optimized considering the average service pressure $\overline{h}$ in the WDN as the objective function to minimize:

$$\overline{h} = \frac{\sum_{i=1}^{n_n} h_i}{n_n} \tag{8}$$

in which h_i and n_n are the pressure head at the generic i-th demand node and the number of demand nodes in the WDN, respectively.

The reduction in service pressure has numerous beneficial effects, including the mitigation of leakage, which is not modelled explicitly in the case study WDN, yearly pipe bursts, and pumping energy consumption.

Assuming that the number of pump models present in the j-th of the n_{ps} pumping station is $n_{m,j}$, the number of decision variables, i.e., the number n_{set} of pump settings to optimize at each time instant, is the following, if a single setting is used for all pumps belonging to the same model in the generic station:

$$n_{set} = \sum_{j=1}^{n_{ps}} n_{m,j} \tag{9}$$

If there is only one pump model in each station ($n_{m,j}$ = 1 for each j), as in the case study network in Figure 1, the relationship (8) simply yields $n_{set} = n_{ps}$.

The following hydraulic constraint concerning the minimum service pressure is considered in the optimization:

$$h_{min} = \min(h_i) \geq h_{des} \tag{10}$$

In the calculations of the present work, the optimization is performed by using the genetic algorithm present in the Matlab® 2023a environment [23], to approximate the optimum in this optimization problem. The hydraulic solver used for each solution proposed by the optimizer is the Epanet 2.2 toolkit developed by [26].

4. Results

Each methodological element described in Section 2 was run on a single unit of a 12th Gen Intel(R) Core(TM) i9-12900H-2.50 GHz. The results of the application to the WDN presented in Section 2 are reported in the following subsections.

4.1. Results of WDN Partitioning

4.1.1. Results of Clustering

The methodology of Creaco et al. (2023) [13] was applied, considering a number M of DMAs equal to 7, as this yields DMA sizes consistent with guidelines on WDN partitioning [3]. For the application of the methodology, a configuration of seven DMAs of the first attempt was manually constructed. Then, the refinement was carried out using the combination of weights reported in the following Table 2. As the clustering was mainly addressed to obtain DMAs with uniform nodal ground elevations inside the single DMA and few boundary pipes, with no focus on the uniformity of demands between DMAs, the weight α_2 was kept equal to 0 in all combinations. Then, four combinations involving values of α_1 and α_3 ranging from 0.1 to 1.9, with sum equal to 2, were considered.

Table 2. Solutions and weights in the clustering. Characteristics of the solutions in terms of number n_b of boundary pipes and modularity contributions H.

Solution	Weights	n_b (-)	H_1 (-)	H_2 (-)	H_3 (-)
1	α_1 = 0.1; α_2 = 0.0; α_3 = 1.9	53	0.0112	0.2351	0.0315
2	α_1 = 0.5; α_2 = 0.0; α_3 = 1.5	50	0.0105	0.1668	0.0468
3	α_1 = 1.0; α_2 = 0.0; α_3 = 1.0	46	0.0097	0.1643	0.0478
4	α_1 = 1.5; α_2 = 0.0; α_3 = 0.5	42	0.0089	0.1642	0.0494

As Table 2 shows, the increase in α_1 at the expense of α_3 tends to produce clustering solutions with progressively smaller values of H_1 (less numerous boundary pipes n_b) and larger values of H_3 (higher heterogeneity of ground elevations inside each DMA) (see also Figure 4). Though not controlled in the refinement process due to α_2 = 0, an improvement in the uniformity of DMA demands (decrease in H_2) is also obtained.

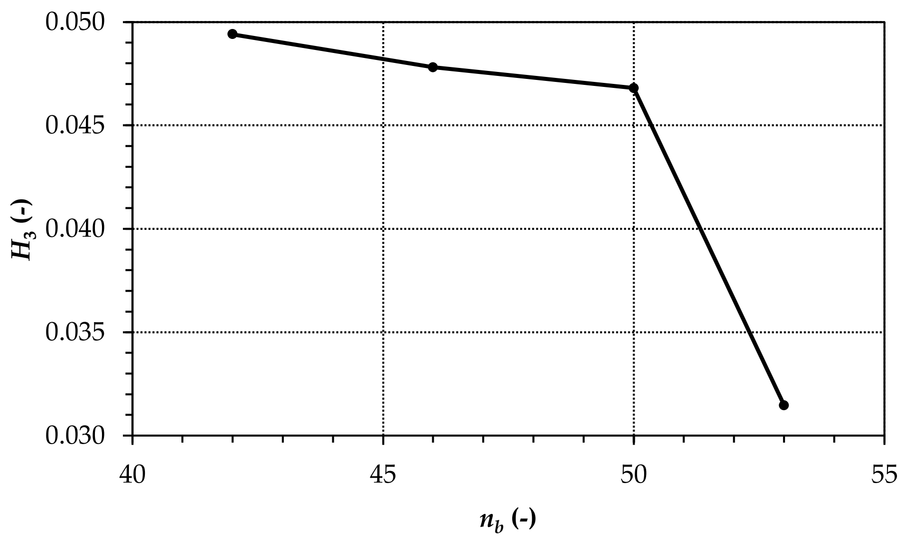

Figure 4. H_3 as a function of n_b for the solutions obtained in the clustering.

The layouts of the four clustering configurations described in Table 2 and Figure 4 are shown in Figure 5. Overall, all solutions seem to fit the altimetric areas present in Figure 1. Though solution 1 marks an outstanding improvement in terms of H_3 compared to the other solutions, one of the DMAs, i.e., the one in magenta, degenerates into a single node. Then, it was discarded in the subsequent analyses. As solutions 2 and 3 are very similar in terms of n_b, H_1 and H_3, only solution 3 was considered for the dividing, together with solution 4.

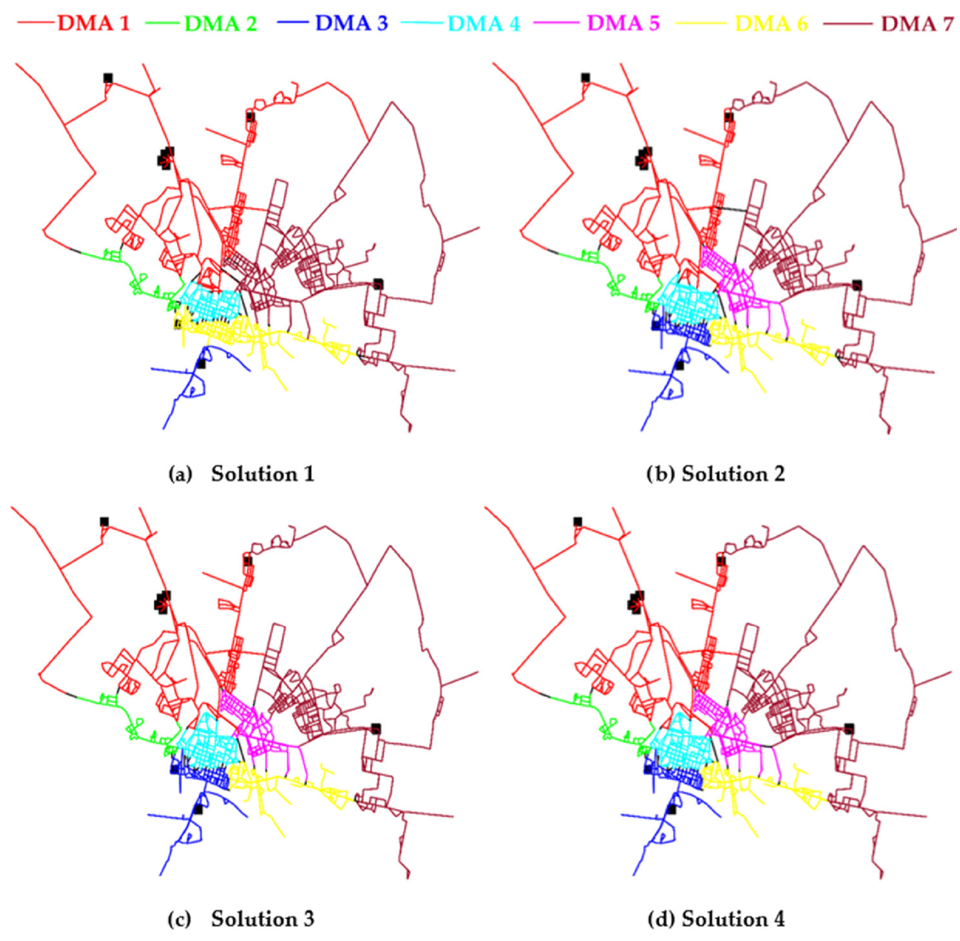

Figure 5. Layout of the clustering solutions.

4.1.2. Results of Dividing

The iterative algorithm described in Section 3.1.2 was applied to clustering solutions 3 and 4, yielding the Pareto fronts in the trade-off between the number of closed isolation valves on boundary pipes $N_{civ} = n_b - n_f$ and GRF, shown in Figure 6a,b, respectively. In these calculations, the desired pressure head h_{des} was considered equal to 20 m.

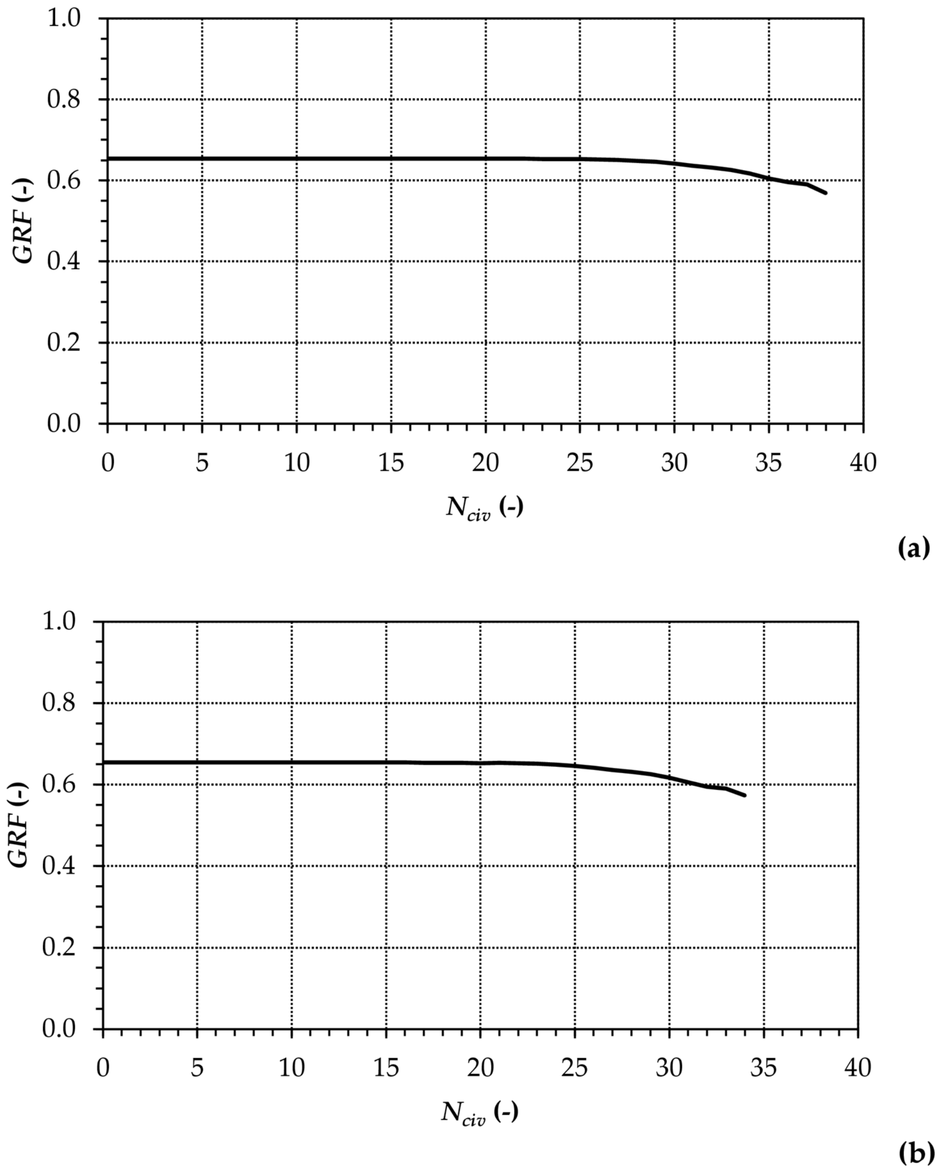

Figure 6. Pareto fronts of solutions in the trade-off between N_{civ} and *GRF*, obtained in the dividing of solutions (**a**) 3 and (**b**) 4.

The curves GRF(N_{civ}) exist for values of N_{civ} ranging from 0 to 38 (solution 3—Figure 6a) or 34 (solution 4—Figure 6b), as the closure of additional isolation valves on boundary pipes causes topological disconnections in the WDN. Expectedly, the two graphs show that GRF tends to decrease as N_{civ} increases, as the closure of isolation valves always causes an increase in head losses and the lowering of service pressure in the WDN. However, the decrease in GRF is almost inappreciable until N_{civ} = 30 for solution 3 (see Figure 6a) or N_{civ} = 25 for solution 4 (see Figure 6b). To the right of these values, the decrease in GRF is appreciable, but still small. As nodal pressure heads never fall below h_{des}, the extreme configurations to the right-hand side were selected as the ultimate partitioning corresponding to a similar value of GRF $\approx$ 0.57 and to values N_{civ} = 38 and N_{civ} = 34 for solutions 3 and 4, respectively. The choice of the configurations with the highest N_{civ} is due to (i) the small decrease in GRF in comparison with the unpartitioned solution (GRF ≈ 0.65), and to (ii) the possibility of limiting the number of flow meters $n_f = n_b - N_{civ}$. In fact, the number of flow meters is then $n_f = n_b - N_{civ} = 8$ for both solutions 3 and 4, which is reasonable for a number M of DMAs equal to 7, to be added to the six flow meters already present at the exit of the pumping stations.

The choice of the feasible partitioning configurations with the highest values of N_{civ} is motivated by the need to limit partitioning costs, as the closure of an isolation valve (following its installation if the valve is absent) is much less expensive than the installation of a flow meter.

4.2. Results of the Optimization of Pump Settings

The methodology described in Section 3.2 was applied to the WDN partitioning solutions obtained at the end of Section 3.1, while assuming that the fixed pumps currently present in the WDN were equipped with the variable speed drive. The following Tables 3 and 4 report the hourly speed settings obtained for the pump stations in solutions 3 and 4, respectively.

Table 3. Settings adopted in the pumping stations in solution 3.

Time (h)	Setting in Station 1	Setting in Station 2	Setting in Station 3	Setting in Station 4	Setting in Station 5	Setting in Station 6
0–1	0.648	0.607	0.754	0.770	0.717	0.571
1–2	0.646	0.607	0.760	0.776	0.708	0.569
2–3	0.648	0.606	0.756	0.774	0.715	0.569
3–4	0.648	0.606	0.756	0.774	0.715	0.569
4–5	0.646	0.615	0.750	0.764	0.780	0.569
5–6	0.707	0.729	0.678	0.710	0.680	0.728
6–7	0.880	0.893	0.943	0.665	0.643	0.909
7–8	0.884	0.939	0.890	0.790	0.673	0.943
8–9	0.880	0.893	0.943	0.665	0.643	0.909
9–10	0.769	0.774	0.786	0.656	0.740	0.798
10–11	0.769	0.774	0.786	0.656	0.740	0.798
11–12	0.777	0.795	0.806	0.725	0.888	0.831
12–13	0.717	0.751	0.738	0.663	0.725	0.765
13–14	0.707	0.729	0.678	0.710	0.680	0.728
14–15	0.672	0.667	0.702	0.702	0.663	0.631
15–16	0.699	0.686	0.761	0.779	0.658	0.648
16–17	0.714	0.707	0.646	0.721	0.671	0.703
17–18	0.717	0.751	0.738	0.663	0.725	0.765
18–19	0.694	0.716	0.729	0.717	0.708	0.706
19–20	0.653	0.659	0.734	0.734	0.638	0.610
20–21	0.652	0.647	0.730	0.740	0.702	0.597
21–22	0.636	0.619	0.748	0.756	0.791	0.572
22–23	0.640	0.613	0.758	0.769	0.736	0.571
23–24	0.649	0.605	0.730	0.733	0.719	0.571

By using the results obtained with the EPANET toolkit [23], the following Figure 7 shows the hourly pattern of minimum (h_{min}) and average ($\bar{h}$) service pressure for solutions 3 and 4 on a typical day of operation, in comparison with the pattern obtained in the benchmark WDN configuration with no partitioning and no pump setting optimization. The analysis of this figure highlights a significant reduction in terms of service pressure. The comparison of solutions 3 and 4 points out that solution 3 enables better mitigation of $\bar{h}$, as a result of more uniform nodal ground elevations inside each DMA. However, the pattern of h_{min} is constant at 20 m for both solutions, due to the minimum pressure constraint adopted in the optimization. Overall, solution 3 enables the reduction in the average and minimum service pressure by 48% and 55%, respectively. Solution 4, instead, enables a reduction in the average and minimum service pressure by 46% and 55%, respectively.

Table 4. Settings adopted in the pumping stations in solution 4.

Time (h)	Setting in Station 1	Setting in Station 2	Setting in Station 3	Setting in Station 4	Setting in Station 5	Setting in Station 6
0–1	0.648	0.606	0.756	0.769	0.716	0.571
1–2	0.658	0.604	0.760	0.778	0.713	0.569
2–3	0.649	0.605	0.760	0.776	0.721	0.569
3–4	0.649	0.605	0.760	0.776	0.721	0.569
4–5	0.642	0.615	0.750	0.758	0.773	0.571
5–6	0.829	0.730	0.765	0.763	0.763	0.729
6–7	0.873	0.890	0.886	0.860	0.786	0.979
7–8	0.944	0.938	0.976	0.985	0.744	0.999
8–9	0.873	0.890	0.886	0.860	0.786	0.979
9–10	0.766	0.792	0.832	0.811	0.639	0.820
10–11	0.766	0.792	0.832	0.811	0.639	0.820
11–12	0.754	0.823	0.697	0.723	0.649	0.922
12–13	0.735	0.763	0.839	0.745	0.659	0.776
13–14	0.829	0.730	0.765	0.763	0.763	0.729
14–15	0.662	0.667	0.705	0.715	0.765	0.607
15–16	0.670	0.692	0.739	0.803	0.665	0.623
16–17	0.742	0.713	0.824	0.849	0.683	0.648
17–18	0.735	0.763	0.839	0.745	0.659	0.776
18–19	0.696	0.727	0.815	0.890	0.639	0.669
19–20	0.677	0.656	0.804	0.798	0.815	0.592
20–21	0.674	0.651	0.732	0.740	0.715	0.601
21–22	0.637	0.623	0.768	0.764	0.791	0.572
22–23	0.645	0.612	0.758	0.764	0.742	0.571
23–24	0.648	0.606	0.756	0.769	0.716	0.571

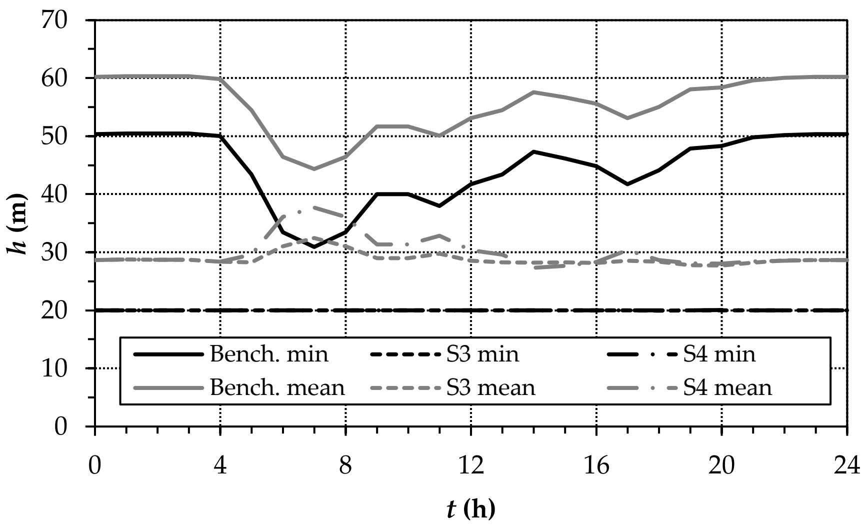

Figure 7. Daily pattern of minimum and mean pressure in the WDN in the benchmark unpartitioned layout and in partitioned solutions 3 and 4.

The following Table 5 points out the effects of WDN partitioning and pump setting optimization in terms of daily average power consumption in the six pumping stations.

In comparison with the benchmark WDN model, solutions 3 and 4 enable reducing power consumption by about 54% and 52%, respectively, in each single station and at WDN scale. Due the more effective service pressure regulation, solution 3 yields a slightly better reduction in the pump power consumption.

Table 5. Mean power (KW) absorbed in each pumping station and in the whole WDN, in the benchmark unpartitioned layout and in partitioned solutions 3 and 4.

Station	Benchmark	Solution 3	Solution 4
Station 1	29.62	11.40	12.10
Station 2	138.95	66.17	67.29
Station 3	19.71	9.00	9.92
Station 4	19.25	7.49	9.84
Station 5	30.22	13.45	12.24
Station 6	145.64	67.62	71.69
Total	383.40	175.13	183.08

As an additional analysis, solutions 3 and 4 were compared in terms of daily average mean pressure h_{mean} and daily average total absorbed energy, with a solution of WDN partitioning into seven districts obtained via clustering based on the Girvan and Newman [27] algorithm, with no consideration of WDN altimetry. The dividing described in Section 3.1.2 was applied to this solution, resulting in n_f = 9 of the n_b = 28 boundary pipes to be equipped with the flow meter, in order to obtain a similar GRF to solutions 3 and 4 under peak demand conditions. Then, the optimization of pump settings was performed as explained in 3.2. Overall, Table 6 proves the solution based on the Girvan and Newman [27] algorithm to be less effective than solutions 3 and 4 in terms of the mitigation of service pressure and energy consumption. This attests to the benefits of performing the clustering while pursuing the uniformity of nodal ground elevations inside each DMA.

Table 6. Comparison of solution 3, solution 4 and the solution based on clustering [27] in terms of daily average mean pressure h_{mean} and total mean absorbed energy.

Results	Solution 3	Solution 4	Solution Based on Clustering [27]
h_{mean} (m)	28.88	30.09	30.83
Total Energy (KW)	175.13	183.08	213.21

5. Discussion

The scientific literature reports numerous works on WDN partitioning. The uniformity of DMAs, in most cases expressed in terms of size or demand, is often sought after. By using the formulation of modularity recently proposed by Creaco et al. [13], this paper shows that an effective WDN clustering into DMAs can also be achieved by pursuing the uniformity of nodal ground elevations inside each DMA, in such a way that the DMAs reflect the altimetric areas of the WDN.

Another novel aspect of the present work concerns the dividing of the WDN into DMAs following the clustering. The choice of which boundary pipes to close or alternatively fit with a flow meter to monitor inter-DMA flow exchanges, and then to derive DMA water consumption, is made using a novel efficient and effective algorithm. Starting from the condition of all open boundary pipes (and then fitted with the flow meter), this algorithm operates by closing them one by one until the closure causes pressure drops below the minimum desired pressure head or topological disconnections from WDN sources. By plotting the number of boundary pipes closed (or fitted with a flow meter) versus the reliability of the WDN in each step of the algorithm, an approximation of the Pareto front of optimal solutions in the trade-off between these two variables is obtained, from which water utility managers can select the ultimate dividing solutions by making economic and reliability considerations.

As the case study WDN is a closed system serving the city of Pavia, in which water is pumped directly from underground wells to WDN users with no intermediate tank(s), a methodology is proposed for the conversion of fixed-speed pumps to variable-speed pumps and for the optimization of pump settings to mitigate service pressure and to reduce the pumping energy consumption in the WDN as a result. While four solutions were obtained in the clustering of the WDN, two of them were further processed for the dividing and for the optimization of hourly pump settings. In the calculations of the present work, the better of the two solutions enabled a reduction in average service pressure, minimum service pressure and pump energy consumption by 48%, 55% and 54%, respectively. Overall, attractive benefits up to about 50% were therefore obtained in terms of reduction in service pressure and energy consumption.

Hydraulic simulations of the present work were carried out considering (as simplifying assumptions) demand-driven outflows, with no dependence on service pressure, and demands lumped to WDN nodes. Nevertheless, the effects of these assumptions are predicted to be small, due to the following considerations:

- The modelled service pressure remained above the threshold of 20 m for full demand satisfaction.
- The rate of leakage in the real WDN is currently small.
- The number of nodes in the WDN layout is high, meaning that demand is always modelled close to its associated user along the pipe.

Future work will be dedicated to extending the model to remove the simplifying assumptions mentioned above, taking inspiration from existing works [28–30].

Future work will also be dedicated to extending the developed methodology to the case of WDN equipped with intermediate tanks.

Author Contributions: Conceptualization, E.C.; methodology, C.G. and E.C.; investigation, A.T., C.G. and E.C.; writing—original draft preparation, E.C. and C.G.; writing—review and editing, A.T.; supervision, E.C.; funding acquisition, E.C. All authors have read and agreed to the published version of the manuscript.

Funding: This research received no external funding.

Data Availability Statement: The data and results of this work may be made available upon reasonable request to the corresponding author.

Acknowledgments: Support from Italian MIUR and University of Pavia is acknowledged within the program Dipartimenti di Eccellenza 2023–2027.

Conflicts of Interest: The authors declare no conflict of interest.

References

1. IEA. *World Energy Outlook 2016—Special Report: Water-Energy Nexus*; IEA: Paris, France, 2016.
2. UK Water Industry Research Limited. *A Manual of DMA Practice*; UK Water Industry Research Limited: London, UK, 1999.
3. Morrison, J.; Tooms, S.; Rogers, D. *DMAs Guidance Notes*; Water Loss Task Force; IWA Publications: London, UK, 2007.
4. Campbell, E.; Izquierdo, J.; Montalvo, I.; Pérez-García, R. A novel water supply network sectorization methodology based on a complete economic analysis, including uncertainties. *Water* **2016**, *8*, 179. [CrossRef]
5. Ciaponi, C.; Creaco, E.; Di Nardo, A.; Di Natale, M.; Giudicianni, C.; Musmarra, D.; Santonastaso, G.F. Reducing impacts of contamination in water distribution networks: A combined strategy based on network partitioning and installation of water quality sensors. *Water* **2019**, *11*, 1315. [CrossRef]
6. Giudicianni, C.; Herrera, M.; Di Nardo, A.; Adeyeye, K. Automatic multiscale approach for water networks partitioning into dynamic district metered areas. *Water Resour. Manag.* **2020**, *34*, 835–848. [CrossRef]
7. Gomes, R.; Sá Marques, A.; Sousa, J. Identification of the optimal entry points at District Metered Areas and implementation of pressure management. *Urban Water J.* **2012**, *9*, 365–384. [CrossRef]
8. Khoa Bui, X.; Marlim, M.S.; Kang, D. Water network partitioning into district metered areas: A state-of-the-art review. *Water* **2020**, *12*, 1002. [CrossRef]
9. Giustolisi, O.; Ridolfi, L. A novel infrastructure modularity index for the segmentation of water distribution networks. *Water Resour. Res.* **2014**, *50*, 7648–7661. [CrossRef]
10. Creaco, E.; Haidar, H. Multiobjective optimization of control valve installation and DMA creation for reducing leakage in water distribution networks. *J. Water Resour. Plan. Manag.* **2019**, *145*, 04019046. [CrossRef]
11. Sharma, A.N.; Dongre, S.R.; Gupta, R.; Ormsbee, L. Multiphase procedure for identifying district metered areas in water distribution networks using community detection, NSGA-III optimization, and multiple attribute decision making. *J. Water Resour. Plan. Manag.* **2022**, *148*, 4022040. [CrossRef]

12. Clauset, A.; Newman, M.E.J.; Moore, C. Finding community structure in very large networks. *Phys. Rev. E* **2004**, *70*, 66111. [CrossRef] [PubMed]
13. Creaco, E.; Giudicianni, C.; Mottahedin, A. Improved community detection for WDN partitioning in the dual topology based on segments and valves. *J. Hydroinformatics* **2023**, *25*, 1341–1357. [CrossRef]
14. Hajebi, S.; Temate, S.; Barrett, S.; Clarke, A.; Clarke, S. Water distribution network sectorisation using structural graph partitioning and multi-objective optimization. *Procedia Eng.* **2014**, *89*, 1144–1151. [CrossRef]
15. Brentan, B.M.; Campbell, E.; Meirelles, G.L.; Luvizotto, E.; Izquierdo, J. Social network community detection for DMA creation: Criteria analysis through multilevel optimization. *Math. Probl. Eng.* **2018**, *144*, 9053238. [CrossRef]
16. Li, W.; Huang, Y.; Ji, L.; Ma, L.; Agarwal, R.K.; Awais, M. Prediction model for energy conversion characteristics during transient processes in a mixed-flow pump. *Energy* **2023**, *271*, 127082. [CrossRef]
17. Li, W.; Huang, Y.; Ji, L.; Zhong, L.; Shi, W.; Zhu, Y. Mechanism and propagation characteristics of rotating stall in a mixed-flow pump. *Renew. Energy* **2020**, *153*, 74–92. [CrossRef]
18. Mansouri, S.A.; Paredes, A.; González, J.M.; Aguado, J.A. A three-layer game theoretic-based strategy for optimal scheduling of microgrids by leveraging a dynamic demand response program designer to unlock the potential of smart buildings and electric vehicle fleets. *Appl. Energy* **2023**, *347*, 121440. [CrossRef]
19. Mansouri, S.A.; Nematbakhsh, E.; Jordehi, A.R.; Marzband, M.; Tostado-Véliz, M.; Jurado, F. An interval-based nested optimization framework for deriving flexibility from smart buildings and electric vehicle fleets in the TSO-DSO coordination. *Appl. Energy* **2023**, *341*, 121062. [CrossRef]
20. Marchi, A.; Simpson, A.R.; Ertugrul, N. Assessing variable speed pump efficiency in water distribution systems. *Drink. Water Eng. Sci.* **2012**, *5*, 15–21. [CrossRef]
21. Rossman, L.; Woo, H.; Tryby, M.; Shang, F.; Janke, R.; Haxton, T. *EPANET 2.2 User Manual*; EPA/600/R-20/133; U.S. Environmental Protection Agency: Washington, DC, USA, 2020.
22. Laarhoven, P.J.M.; Aarts, E.H.L. *Simulated Annealing: Theory and Applications*; D. Reidel: Dordrecht, The Netherlands, 1987; ISBN 90-277-2513-6.
23. *MATLAB*, version: 9.14.0 (R2023a); The MathWorks, Inc.: Natick, MA, USA, 2023.
24. Creaco, E.; Zheng, F.; Pezzinga, G. Minimum transport driven algorithm for water distribution network partitioning. Aqua-Water Infrastruct. *Ecosyst. Soc.* **2022**, *71*, 120–138.
25. Creaco, E.; Franchini, M.; Todini, E. Generalized resilience and failure indices for use with pressure-driven modeling and leakage. *J. Water Resour. Plan. Manag.* **2016**, *142*, 04016019. [CrossRef]
26. Eliades, D.G.; Kyriakou, M.; Vrachimis, S. Polycarpou MMEPANET-MATLABToolkit: An Open-Source Software for Interfacing EPANET with, MATLAB. In Proceedings of the 14th International Conference on Computing and Control for the Water Industry (CCWI), Amsterdam, The Netherlands, 7–9 November 2016; p. 8. [CrossRef]
27. Girvan, M.; Newman, M.E. Community structure in social and biological networks. *Proc. Natl. Acad. Sci. USA* **2002**, *99*, 7821–7826. [CrossRef]
28. Menapace, A.; Avesani, D. Global Gradient Algorithm Extension to Distributed Pressure Driven Pipe Demand Model. *Water Resour. Manag.* **2019**, *33*, 1717–1736. [CrossRef]
29. Avesani, D.; Righetti, M.; Righetti, D.; Bertola, P. The extension of EPANET source code to simulate unsteady flow in water distribution networks with variable head tanks. *J. Hydroinform.* **2012**, *14*, 960–973. [CrossRef]
30. Berardi, L.; Giustolisi, O.; Todini, E. Accounting for uniformly distributed pipe demand in WDN analysis: Enhanced GGA. *Urban Water J.* **2010**, *7*, 243–255. [CrossRef]

Disclaimer/Publisher's Note: The statements, opinions and data contained in all publications are solely those of the individual author(s) and contributor(s) and not of MDPI and/or the editor(s). MDPI and/or the editor(s) disclaim responsibility for any injury to people or property resulting from any ideas, methods, instructions or products referred to in the content.